P1.6 **Simulation of the impact of new aircraft and satellite-based ocean surface wind measurements on H*Wind analyses**

Timothy L. Miller[1], R. Atlas[2], P. G. Black[3], J. L. Case[4], S. S. Chen[5], R. E. Hood[1], J. W. Johnson[6], L. Jones[6], C. S. Ruf[7], and E. W. Uhlhorn[2]

[1]NASA/MSFC, Huntsville, AL
[2]NOAA/AOML, Miami, FL
[3]Naval Research Laboratory, Monterey, CA
[4]ENSCO Inc./Short-term Prediction Research and Transition (SPoRT) Center, Huntsville, AL
[5]University of Miami, Miami, FL
[6]University of Central Florida, Orlando, FL
[7]University of Michigan, Ann Arbor, MI

1. Introduction

Accurate observations of surface ocean vector winds (OVW) with high spatial and temporal resolution are required for understanding and predicting tropical cyclones. As NASA's QuikSCAT and Navy's WindSat operate beyond their design life, many members of the weather and climate science communities recognize the importance of developing new observational technologies and strategies to meet the essential need for OVW information to improve hurricane intensity and location forecasts. The Hurricane Imaging Radiometer (HIRAD) is an innovative technology development which offers new and unique remotely sensed satellite observations of both extreme oceanic wind events and heavy precipitation. It is based on the airborne Stepped Frequency Microwave Radiometer (SFMR), which is the only proven remote sensing technique for observing tropical cyclone (TC) ocean surface wind speeds and rain rates. The proposed HIRAD instrument advances beyond the current nadir viewing SFMR to an equivalent wide-swath SFMR imager using passive microwave synthetic thinned aperture radiometer (STAR) technology. This sensor will operate over 4-7 GHz (C-band frequencies) where the required TC remote sensing physics has been validated by both SFMR and WindSat radiometers. The instrument is described in more detail in a paper by Jones *et al.* (JP1.18) presented to the Tropical Meteorology Special Symposium at this AMS Annual Meeting.

2. HIRAD Observing System Simulation Experiments

Simulations of HIRAD passes through a numerical forecast of hurricane Frances have been developed to demonstrate HIRAD estimation of surface wind speed over a wide swath in the presence of heavy rain. These are currently being used in "quick" OSSEs (Observing System Simulation Experiments) with H*Wind analyses as the discriminating tool. The H*Wind analysis, a product of the Hurricane Research Division of NOAA's Atlantic Oceanographic and Meteorological Laboratory, brings together wind measurements from a variety of observation platforms into an objective analysis of the distribution of wind speeds in a tropical cyclone. This product is designed to improve understanding of the extent and strength of the wind field, and to improve the assessment of hurricane intensity. Refer to http://www.aoml.noaa.gov/hrd/data_sub/wind.html for more details on the H*Wind analysis product.

Observation Simulated	Comment
QuikSCAT	
SFMR (aircraft ocean surface winds sensor)	Winds along ground track; no cross-track structure
Flight-level winds	
Dropsonde winds	Drops in eyewall and at storm center from aircraft
Airborne Doppler Radar	Future work
GOES cloud winds	Using actual data for location (relative to storm center), nature run data plus error for wind values
Buoys, ships, coastal sensors	
HIRAD	3 aircraft altitudes, satellite

Table 1. List of observations simulated from nature run.

[1] Corresponding author address: Timothy L. Miller, NASA/MSFC, Earth Science Office, Huntsville, AL 35812; e-mail: tim.miller@nasa.gov

Observations have been simulated from both aircraft altitudes and space (see Table 1). The simulated flight patterns for the aircraft platform cases have been designed to duplicate the timing and flight patterns used in routine NOAA and USAF hurricane surveillance flights, and the spaceborne case simulates a TRMM orbit and altitude.

For the nature run from which the observations are simulated, we chose to use a numerical forecast from the state-of-the-art system described by Chen *et al.* (2007). The storm simulated is Hurricane Frances (late August of 2004) using a system of nested grids with the innermost one having a horizontal grid spacing of 0.015 degrees (~1.6 km) in longitude and latitude. The model is non-hydrostatic in the atmosphere with detailed explicit microphysics and an interactive ocean wave model. The results include a realistic eyewall, rainbands and other convective and mesoscale structure (Fig. 1).

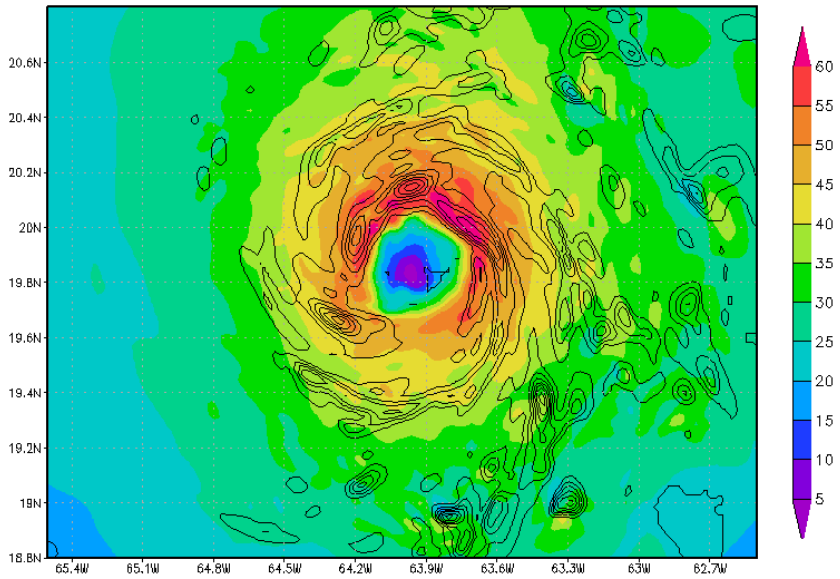

Fig. 1. Near-surface wind speed (m s^{-1}) as modeled for Hurricane Frances at 1800 UTC on 31 August, 2004. Wind speed is represented by the color scale, and rain rate with solid contours (interval = 20 mm hr^{-1}). Only a portion of the inner-most grid is shown.

The HIRAD sampling, as currently implemented, constructs cross-track scans with each gridded wind speed value so that the spatial resolution over the HIRAD field-of-view is of the same size as the model grid both cross-track and along track. (This resolution is of similar size, but not exactly the same as the planned instrument.) Contiguous scans are formed along the track in a pushbroom fashion as the platform flies along. Both “Figure-4” and “Butterfly” patterns, which provide 2 and 3 passes through the eye, respectively, have been simulated for the aircraft cases and a single pass was simulated in the spaceborne case (at 5-km resolution). Surface averaging over realistic antenna beam resolution cells will be added to the surface sampling simulations in the future. The HIRAD cross-track field-of-view is approximately ± 60° which translates to a swath width of ~70 km at the highest aircraft altitude considered, which is 20 km for a typical ER-2 flight. In the satellite case the swath was approximately 2000 km for an orbit altitude of 450 km. In the satellite simulation chosen, the satellite ground track passed through the hurricane eye, and for this example the limited modeled wind field occupied only ± 45° of the available HIRAD field-of-view.

Since the modeled surface wind fields are provided on 1-hour increments, time interpolated wind fields are used in the surface sampling. The time interpolation is done using storm centric 1-hour data over the duration of the aircraft flight patterns, which take approximately 1.5–2 hours to complete. This technique was used for all of the simulated observations.

Errors that are representative of the particular instrument were added to the simulated observations. For HIRAD, wind speed errors were simulated using a simplified model that was calibrated with SFMR errors in estimating actual hurricane winds. The total SFMR error was separated into a surface component, rain free approximation, and an atmospheric component, where the standard deviation of the total error was the vector sum of these two quantities. Since SFMR is nadir viewing, the standard deviation of the HIRAD error was modeled by applying a $\sec\theta$ dependence to the atmospheric component. For each simulation case, this model was used in a single trial way to produce pixel-by-pixel wind speed errors that were a function of modeled rain rate and viewing angle over the swath.

Since this single trial method produces a few large errors in each simulation that can skew the H*Wind results, a 2-sigma limit was applied to each random error and a 3x3 median filter was applied to the resultant wind field.

QuikSCAT observations were simulated as follows. The objective is to simulate a QuikSCAT hurricane observation that is statistically representative of actual QuikSCAT hurricane measurements of ocean vector winds. The simulated results provide similar spatial sampling with reasonable error characteristics (e.g. wind speed saturation for high wind speeds > 30 m/s), contamination of wind speed and wind direction in the presence of rain, etc. The wind speed simulation incorporates a transfer function that is derived from the correlation of QuikSCAT L2B-12.5 km retrieved wind speeds and corresponding QRad rain rates and H*Wind surface analysis for 10 collocated hurricane events (2003–2005). (See Fig. 2 for examples of the distribution of these distributions.) This transfer function, also called *wind speed ratio (WSR)*, is modeled as a ratio of L2B-12.5 km wind speed and H*Wind surface wind speed with respect to QRad rain rate (R), represented symbolically as follows:

$$WSR = f(L2B\ 12.5, H*Wind, R)$$

Given a nature-run surface wind and rain fields, we compute the wind speed ratio. The simulated QuikSCAT wind speed retrieval is the product of this *WSR* and the nature-run surface wind speed ($Wspd_{truth}$).

$$QSCAT_{wind} = WSR \times Wspd_{truth}$$

To simulate the QuikSCAT random wind speed retrieval error, zero-mean Gaussian noise is added to the simulated wind speed with the standard deviation increasing with wind speed. Although a perfect simulation for any pixel is impossible to achieve, the simulated wind speed field resembles actual QuikSCAT observations both by spatial patterns and statistics. An example of the simulation wind speeds is shown in Figure 2 for a nature-run of Hurricane Frances, along with actual QuikSCAT measurements for three hurricane over-flights.

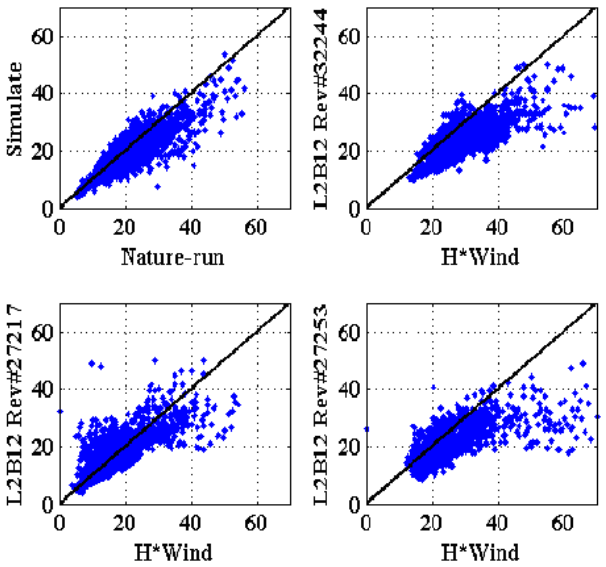

Fig.2 Comparison between simulated hurricane wind speed retrieval (upper left) to three actual QuikSCAT hurricane wind speed retrievals for Hurricane Frances (remaining panels).

For clear sky and light rain, the wind direction simulation incorporates a random retrieved wind direction uncertainty (~18° rms). For heavier rain (> 15 mm hr^{-1}), QuikSCAT wind direction retrievals are cross-swath (independent of actual surface winds). An example of the simulated OVW for Hurricane Frances is shown in Figure 3.

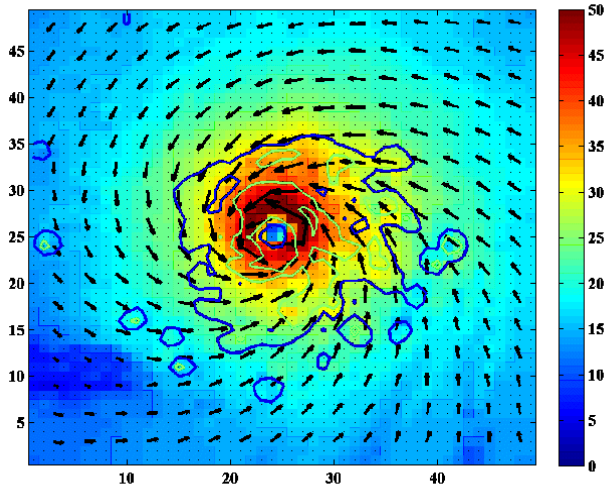

Fig. 3 (a) Hurricane Frances Nature-run OVW's with rain contours.

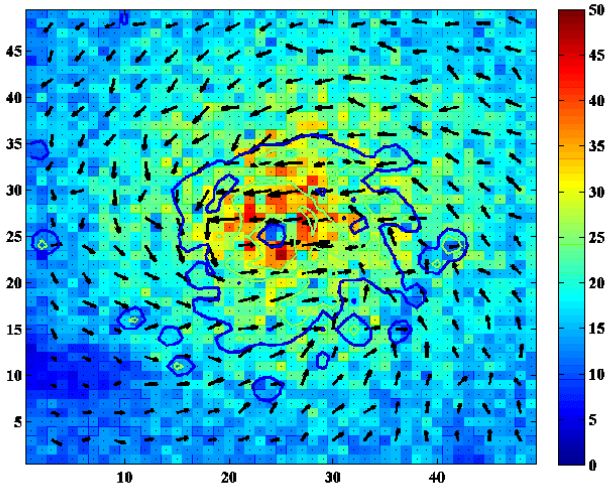

Fig. 3 (b) Simulated QuikSCAT OVW overlaid with nature-run rain contours.

Dropsonde measurements were simulated as being dropped from a typical flight level (3 km), and 3-D trajectories were calculated using the model 3-D winds and assuming an empirical drop rate as a function of height. Spatially (vertically) correlated noise corresponding to turbulence was added to the simulated measurements. Drops were made around the center of the eyewall and in the center of the eye (i.e. 6 drops per Figure-4 flight). Figure 4 shows locations of drops and horizontal trajectories of the dropsondes for one flight leg.

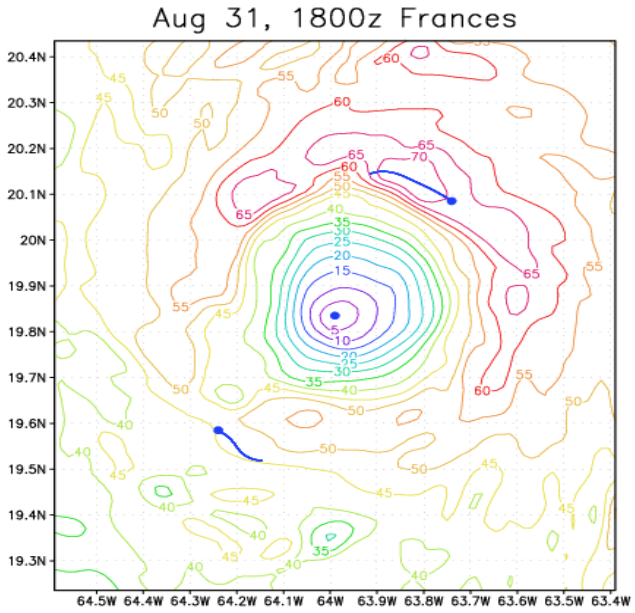

Fig. 4. Nature run flight-level wind speed along with locations of sonde drops (blue circles) and trajectories (blue line) for one aircraft flight leg. Note that in this case, one of the sondes happened to pass through the wind maximum.

GOES cloud winds were simulated by applying a location (horizontal and vertical) template obtained from actual GOES winds during the time period studied, translated horizontally by the difference in locations of the simulated and real storms. The template was then used to interpolate values of the wind vectors from the nature run. The wind components were averaged vertically over 1000 meters to simulate the vertical "smearing" effect of using clouds as tracers, and a random error of sigma 2 m s^{-1} (limited to no more than 20% of the wind speed value) was added to the simulated measurement. Note that the GOES winds were generally distant from the vortex and thus did not have a large influence on the H*Wind analysis.

Buoys and ASOS measurements were simulated by interpolating the nature run winds to the point of measurement, and temporally correlated noise was added to represent turbulence. However, the number and location of these measurements were such that they did not substantially influence the H*Wind analysis.

H*Wind analyses were conducted for various configurations of observations. Because H*Wind is used by the operational community to evaluate the intensity, structure, and location of tropical storms, especially over ocean, the authors believe that an evaluation of the improvement to an H*Wind analysis by any one or set of measurements provides an excellent metric for assessing the relative value of various observations.

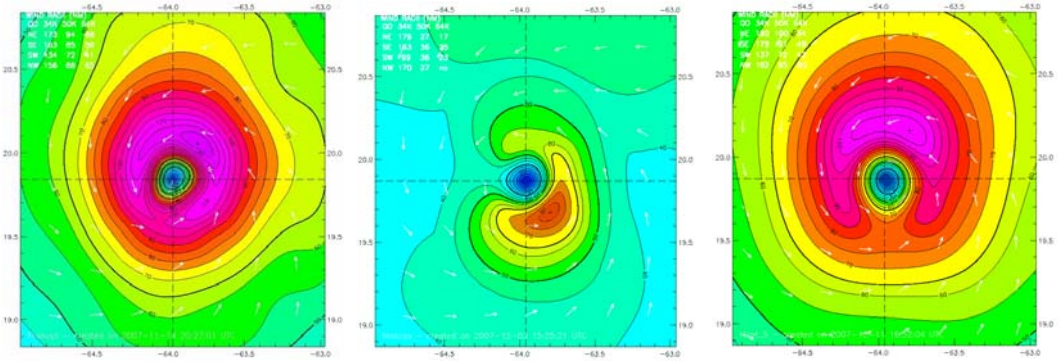

Fig. 5. H*Wind surface wind analyses. (a – left) With full nature run information; (b – center) with current satellites, no aircraft,; (c – right) with HIRAD satellite, no aircraft.

Figure 5a shows the H*Wind analysis when the nature run itself is used as input, and thus represents the "perfect" H*Wind analysis for this case. In comparison with the nature run itself (Fig. 1), the H*Wind analysis does not include much of the smaller-scale structure, but it does capture the maximum wind speed, the gross structure of the wind

field including quadrants of strongest and weakest winds, and the location of the vortex center. Figure 5b shows the H*Wind analysis with no aircraft observations and with current satellite capabilities (QuikSCAT and GOES), while Figure 5c shows the H*Wind analysis again with no aircraft observations, but now with the proposed HIRAD satellite. Since HIRAD is able to observe OVW through heavy rain and high winds, the vortex is much better defined compared to the H*Wind analysis with current satellite capabilities.

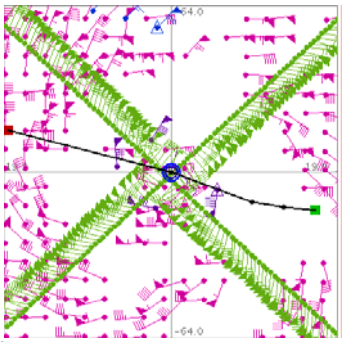

Fig. 6a

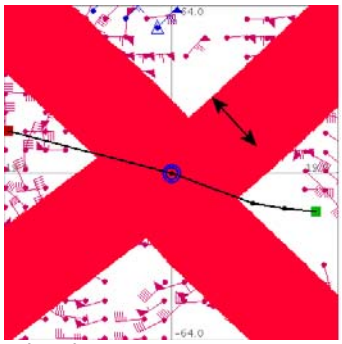

Fig. 6b

Fig. 6 shows the data coverage for two of the aircraft cases, that of SFMR (Fig. 6a) and HIRAD at 11 km (6b). Note that the wind data are shown with wind barbs, and due to the high density of measurements the HIRAD swath appears too large. The double-headed arrow indicates the actual swath width. In the case of SFMR, there is no width to the swath, but rather a line of measurements underneath the flight path. Both cases also include simulated QuikSCAT observations.

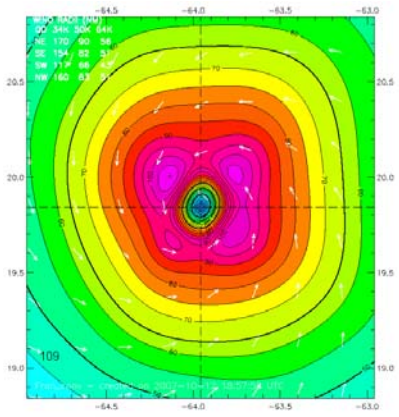

7a. With SFMR

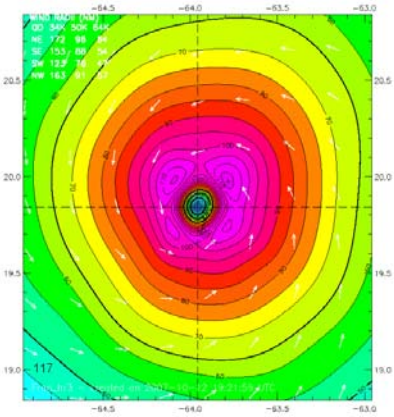

7b. With HIRAD at 3 km.

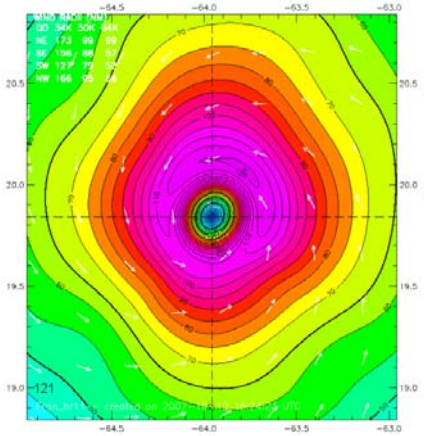

7c. With HIRAD at 11 km

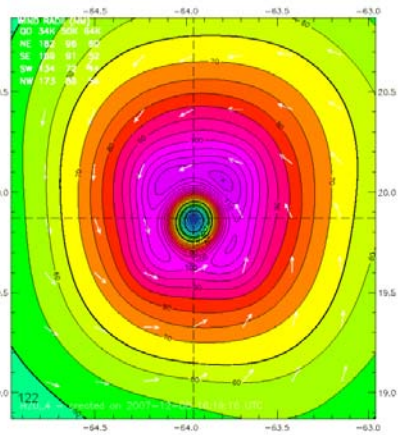

7d. With HIRAD at 20 km

Fig. 7. Simulated H*Wind analyses using the combinations of aircraft observations at various altitudes listed below each panel.

Fig. 7 shows the results of H*Wind analyses with various aircraft configurations: (a) with SFMR; (b) with HIRAD at 3 km; (c) with HIRAD at 11 km; (d) with HIRAD at 20 km. Because H*Wind preserves the maximum wind data point in all cases and random variations cause sporadic results, these analyses do not include random noise added to the data. (Analyses with noise added are of similar appearance, but with varying wind maxima.) Maximum wind values in knots are shown in the lower left corner of each image. As HIRAD is flown at a higher altitude, the swath is wider and hence the advantage in terms of *coverage* is greater. Since H*Wind does not capture high-resolution features in any case (except for the wind maximum itself), the lower spatial resolution as altitude increases does not noticeably degrade the H*Wind analysis, and the vortex structure is generally better defined for the high-altitude HIRAD than it is for the other cases. However, even the lower-altitude HIRAD provides more information than SFMR and thus results in an arguably more realistic analysis. The maximum wind speed using HIRAD is closer to that of the nature run (125 knots) than the SFMR in all instances (with no random noise), and becomes closer as HIRAD increases.

3. Conclusions

The use of data from the proposed HIRAD instrument is shown to improve the quality of the H*Wind analyses in terms of vortex structure and wind maximum in comparison with simulations of current technologies. When the simulated HIRAD is on a low earth orbiting satellite and passes over the storm center, the vortex definition is excellent, although the wind maximum is somewhat below that of the nature run due to spatial resolution lower than that of the convective cells in the storm. When HIRAD is on an aircraft, the improvement in comparison with SFMR is significant, although the size of the improvement depends upon the location of the storm's maximum wind, i.e. whether SFMR is able, with its zero swath width, to capture a wind speed value close to the maximum. The use of HIRAD increases the probability that the wind maximum will be captured.

Reference:

Chen, S. S., J. F. Price, W. Zhao, M. A. Donelan, E. J. Walsh, 2007: The CBLAST-Hurricane Program and the Next-Generation Fully Coupled Atmosphere–Wave–Ocean Models for Hurricane Research and Prediction. *Bull. Amer. Meteor. Soc.,* **88**(3), 311-317.